Measurement of the Rotation Rate in the Deep Solar Interior

S. Tomczyk
High Altitude Observatory, NCAR, P.O. Box 3000, Boulder, CO 80307

J. Schou
Center for Space Physics and Astrophysics, ERL 328, Stanford University, CA 94305

and

M. J. Thompson
Astronomy Unit, Queen Mary and Westfield College, Mile End Road, London E1 4NS, UK

Submitted to Ap. J. Lett.

ABSTRACT

We present a measurement of solar internal rotation based on observations obtained over 3 months in early 1994 with a new instrument called LOWL. This instrument allows for the simultaneous observation of low- and intermediate-degree solar oscillations with spatial resolution. We have measured the frequency splitting of 673 multiplets with degrees ranging from 1 to 80, and inverted these to derive an estimate of the solar internal rotation profile between 0.2 and 0.85 $R_\odot$. The accuracy of this measurement ranges from $\sim$1% in the outer regions to $\sim$5% at 0.2 $R_\odot$ and thus significantly extends helioseismic rotation measurements into the deep solar interior. We confirm earlier findings that near the base of the convection zone the solar rotation profile undergoes a transition from surface-like differential rotation to a rotation rate that is independent of latitude. Additionally, we find that from the base of the convection zone down to 0.2 $R_\odot$ the rotation is constant with radius at a rate somewhat lower than the surface equatorial rate. The accuracy of our measurement in the deep solar interior provides a strong constraint to theories of solar and stellar angular momentum transport.

Subject headings: Sun: oscillations, internal rotation

1. Introduction

Helioseismology has proven to be a powerful diagnostic of the internal structure and rotation of the Sun. Measurements of intermediate-degree rotational frequency splittings by various observers (Duvall, Harvey and Pomerantz, 1986; Brown *et al.*, 1989; Libbrecht, 1989; Rhodes *et al.*, 1990) indicate that throughout the convection zone the solar angular velocity follows a surface-like latitude distribution with a transition to latitude independent rotation near the base of the convective envelope. Below $\sim 0.4 R_\odot$ the solar rotation rate remains highly uncertain due to a lack of accurately measured splittings for low-degree modes. Attempts to measure these splittings using spatially resolved observations have generally failed due to instrumental noise. Observations of the Sun in integrated light have shown the requisite stability to observe low-degree oscillations. However, these observations are unable to discriminate spatially between individual oscillation modes, and therefore require modeling of the blended modes to obtain the splittings. This technique has produced several reports of large low-degree frequency splittings (Claverie *et al.*, 1981; Pallé *et al.*, 1988; Toutain and Fröhlich, 1992) as well as conflicting reports of moderate splittings (Pallé *et al.*, 1990; Loudagh *et al.*, 1993; Toutain and Kosovichev, 1994) resulting in uncertainty about the rotation rate of the deep solar interior. These inconsistent measurements imply that this technique may be subject to significant systematic errors.

This letter presents the initial results from a new instrument which observes both low- and intermediate-degree oscillations with spatial resolution thus providing a reliable estimate of solar internal rotation between 0.2 and $0.85 R_\odot$. In Section 2 we discuss the characteristics of the instrument and the observations. In Section 3 a description is given of the analysis procedure used to obtain the rotational frequency splittings from the data, as well as the inversion technique used to infer the solar internal rotation profiles from the splittings. The results of the inversion are discussed in Section 4 and in Section 5 we conclude with some implications of this measurement for our understanding of solar angular momentum transport.

2. Observations

The observations used in this study were obtained with the recently completed instrument which we call LOWL. The instrument is described in detail elsewhere (Tomczyk *et al.*, 1994), and will be discussed only briefly here. The LOWL is a velocity imaging instrument based on a Potassium Magneto-Optical-Filter (MOF). It obtains full disk images simultaneously in two 2 pm bandpasses displaced ±110 pm into opposite wings of the solar absorption line of Potassium at 769.9 nm. Images are obtained every 15 seconds with a spatial resolution of 25 arcsec and a noise level of 15 m/s/pixel. After correcting the raw images for detector bias and gain variations and image motion, an estimate of the radial velocity v can be estimated at each pixel from

$$v = k\frac{I_b - I_r}{I_b + I_r} + v_0 \tag{1}$$

where k is a calibration constant which has the same units as v, I_b and I_r are the intensities through the blue and red bandpasses, and v_0 is a systematic velocity offset. The calibration constant is determined daily by modeling the spatial variation of the radial velocity across the solar disk due to solar rotation. The velocity variations caused by the relative motions of observer and Sun are removed through an ephemeris calculation. For the present study the velocity images were averaged over 1 minute intervals.

The atomic vapors employed in the MOF make the instrument extremely stable; drift in the instrument zero-point is < 6 cm/s rms integrated over the 5-minute band, allowing solar noise-limited observations down to degree l=0. The dual beam technique ensures that the instrument is insensitive to noise sources arising from intensity fluctuations and image motion, and results in a doppler analyzer with no moving parts. The instrument is located at an altitude of 3414 m on Mauna Loa on the island of Hawaii and became operational on Feb 26, 1994. The observations used for this study consist of 26309 averaged velocity images obtained between Feb. 26 and May 19, 1994, with an overall duty cycle of 22%.

3. Analysis

The averaged velocity images were projected onto spherical harmonics after apodizing the solar image between $0.875R_\odot$ and $0.975R_\odot$ with a cosine bell. For each target (l, m) the time-series of spherical harmonic coefficients were then gap filled with zeros and padded to a length of 120000

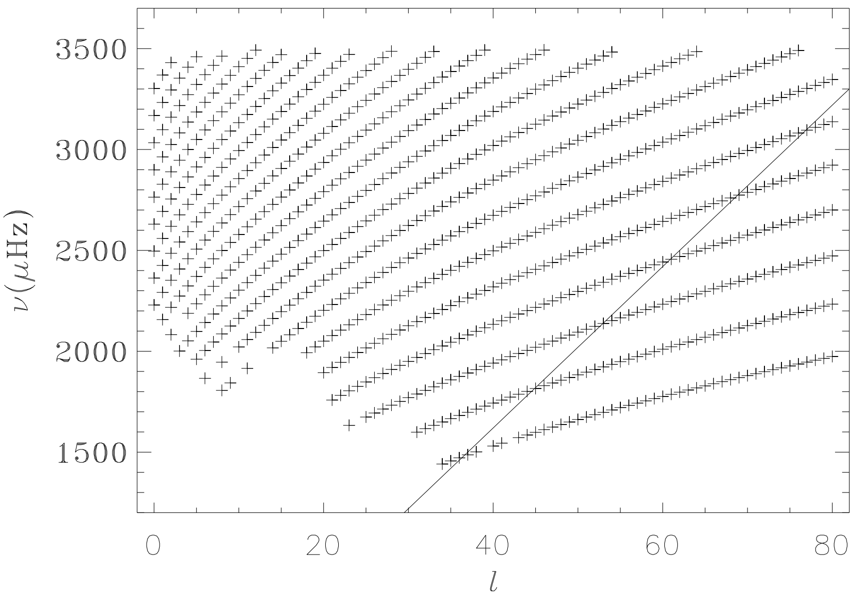

Fig. 1.— $l-\nu$ diagram showing the modes used in this paper. The solid line indicates $\nu/L = 40\mu Hz$.

in order to perform a Fast Fourier Transform. This yields an effective frequency resolution of 0.14μHz. Due to the limited spatial resolution of the instrument only spherical harmonics with degree $l \leq 80$ were used.

Frequency splittings were obtained for each target (l, n) multiplet by simultaneously fitting the Fourier transforms of all m's in the target multiplet (Schou, 1992; 1994). The leakage from other modes due to the incomplete spatial coverage and the temporal sidelobes caused by the low duty cycle were taken into account. Instead of fitting individual mode frequencies, the variation of mode frequency ω_{nlm} with azimuthal order m was expanded as:

$$\omega_{nlm}/2\pi = \nu_{nl} + \sum_{j=1}^{j_{\max}} a_j(n,l) P_j^{(l)}(m), \qquad (2)$$

where ν_{nl} is the average mode frequency, the a_j are the fitted coefficients and the $P_j^{(l)}$ are a set of ortho-normal functions of degree j (Ritzwoller and Lavely, 1991; Schou *et al.* 1994). The set of modes fitted is shown in Figure 1. Figure 2 shows a_1 which describes the linear variation of mode frequency with m and relates to the rotation rate, as a function of ν/L (where $L = \sqrt{l(l+1)}$) which is related to the turning point depth of the mode. The lack of variation of a_1 with ν/L is a preliminary indication of a flat internal rotation profile.

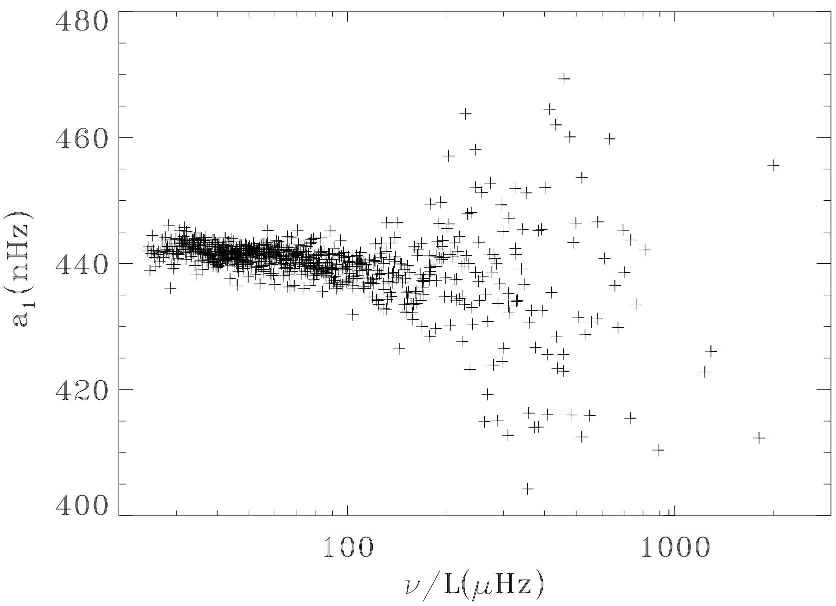

Fig. 2.— a_1 as a function of ν/L. Some modes have splitting outside the range used for this plot.

Having obtained the splitting coefficients, these were then inverted to estimate the Sun's internal rotation rate. The odd a coefficients $a_{2s+1}(n,l)$ are related to the underlying rotation rate

$\Omega(r,\theta)$ by kernels $K^{(a)}_{nls}(r,\theta)$ according to

$$2\pi\ a_{2s+1}(n,l) \;=\; \int_{r,\theta} K^{(a)}_{nls}(r,\theta)\,\Omega(r,\theta)\,r\,\mathrm{d}r\mathrm{d}\theta \;+\; \epsilon_{nls} \tag{3}$$

(Schou *et al.* 1994). The kernels $K^{(a)}_{nls}(r,\theta)$ are functions of the equilibrium structure of the Sun, and are taken to be known. Each ϵ_{nls} is the error in $2\pi a_{2s+1}(n,l)$; the errors are assumed to be independent and normally distributed, with zero mean and standard deviation $\sigma^{(a)}_{nls}$. The North-South symmetric component of the internal rotation rate may be estimated by inverting the constraints (3). A number of different techniques can be used for the inversion: we have employed a 2-D Regularized Least Squares (RLS) inversion method which minimizes

$$\sum_{nls}\left[\frac{\int_{r,\theta} K^{(a)}_{nls}\bar{\Omega} r\mathrm{d}r\mathrm{d}\theta - 2\pi a_{2s+1}(n,l)}{\sigma^{(a)}_{nls}}\right]^2$$
$$+\mu_r \int_{r,\theta} f_r(r,\theta)\left(\frac{\partial^2\bar{\Omega}}{\partial r^2}\right)^2 \mathrm{d}r\mathrm{d}\theta + \mu_\theta \int_{r,\theta} f_\theta(r,\theta)\left(\frac{\partial^2\bar{\Omega}}{\partial\theta^2}\right)^2 \mathrm{d}r\mathrm{d}\theta\,. \tag{4}$$

Here $\bar{\Omega}(r,\theta)$ is the solution, which we represent as a bilinear function on a mesh comprising 24 uniformly spaced intervals in θ and 50 intervals in r spaced approximately uniformly in the acoustical radius. The functions f_r and f_θ are non-negative weights that determine the relative importance of the smoothing constraints at different locations; here we chose them as described in Schou *et al.* (1994). The choice of values for μ_r and μ_θ determines the trade-off between resolution and noise amplification.

In any linear inversion technique it is possible to represent the solution at any point (r_0,θ_0) as a linear combination of the data, i.e. there exist coefficients $c^{(a)}_{nls}(r_0,\theta_0)$ such that

$$\bar{\Omega}(r_0,\theta_0) \;=\; \sum_{nls} c^{(a)}_{nls}(r_0,\theta_0)\,a_{2s+1}(n,l)\,. \tag{5}$$

Combining eqs. (3) and (5) yields

$$\bar{\Omega}(r_0,\theta_0) \;=\; \int_{r,\theta}\mathcal{K}(r_0,\theta_0;r,\theta)\,\Omega(r,\theta)\,r\,\mathrm{d}r\mathrm{d}\theta \;+\; \sum_{nls} c^{(a)}_{nls}(r_0,\theta_0)\,\epsilon_{nls}\,, \tag{6}$$

where the averaging kernel $\mathcal{K}(r_0,\theta_0;r,\theta)$ is defined by

$$\mathcal{K}(r_0,\theta_0;r,\theta) \;=\; \sum_{nls} c^{(a)}_{nls}(r_0,\theta_0)\,K^{(a)}_{nls}(r,\theta)\,. \tag{7}$$

The averaging kernels show how the solution is actually a weighted average of the true solution (plus the term propagated from the data errors) and hence are a useful way of visualizing the resolution of the inversion. An estimate of the random error at a given point can be estimated as

$$\sigma(r_0,\theta_0)^2 = \sum_{nls}\left[c^{(a)}_{nls}(r_0,\theta_0)\sigma^{(a)}_{nls}\right]^2. \tag{8}$$

This is only an estimate of the random error as propagated from the input splittings. The difference between the inferred and the true rotation rate could be much larger due to unresolved features in the true rotation rate.

4. Results

Our dataset comprised 1988 a_1, a_3 and a_5 coefficients for 673 (n, l) multiplets with l ranging from 1 to 80. (For $l = 1$ multiplets only a_1 was fitted, and for $l = 2$ only a_1 and a_3.) This dataset includes only those modes with $\nu/L > 40\mu$Hz. This cut-off was imposed to exclude the most shallowly penetrating modes, whose frequency determinations may be susceptible to systematic error. For the inversion we adopted tradeoff parameter values $\mu_r = 10^{-7}$ and $\mu_\theta = 10^{-3}$ which were chosen to maximize resolution (as given by the extent of the averaging kernels) without allowing the errors to overwhelm the solution. The attainable resolution in the radial direction is generally better than that in the latitudinal direction. This could be improved considerably in the outer parts of the Sun if one were to have more a coefficients per multiplet; with $a_1 - a_5$ there is no possibility of significantly improving the latitudinal resolution by reducing the value of μ_θ (cf. Schou *et al.* 1992).

The rotation rate we infer is shown in Figure 3a with the corresponding formal one standard deviation uncertainties shown in Figure 3b. Throughout most of the solar interior the error level is only a few nHz, rising to 10 nHz at $r \approx 0.3R_\odot$ and to 25 nHz at $r \approx 0.2R_\odot$. The solution and its level of uncertainty is illustrated again in Figure 4, which shows cuts through the inferred rotation rate at colatitudes $\theta = 0°$, 45° and 90°.

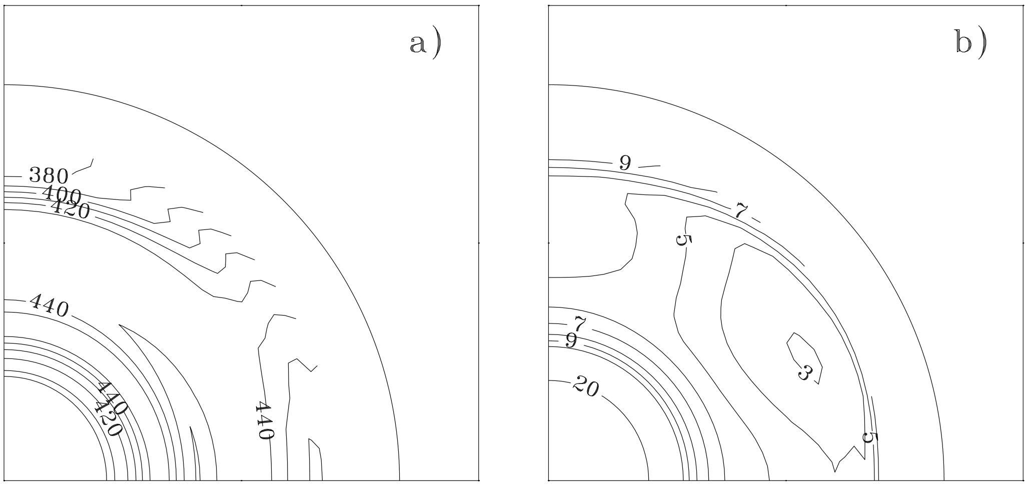

Fig. 3.— (a) The solar rotation rate between $r = 0.2R_\odot$ and $r = 0.85R_\odot$, as inferred using the 2-D RLS technique with $\mu_r = 10^{-7}$, $\mu_\theta = 10^{-3}$. The contour spacing is 10 nHz. (b) The corresponding 1-σ error levels (values are in nHz).

In the convection zone we see significant radial variation in the rotation rate in a transition from surface-like differential rotation to a rotation rate that is independent of latitude. This is in basic agreement with previous findings (Christensen-Dalsgaard and Schou, 1988; Brown *et al.*, 1989). The differential rotation vanishes at a depth of $\sim$0.65 $R_\odot$ which is consistent with recent helioseismological estimates of the base of the convection zone (Christensen-Dalsgaard *et al.*, 1991) to within the resolution of our inversion. Below $r \approx 0.65 R_\odot$ we find no significant variation of the rotation rate with radius. The local maximum at $r \approx 0.4 R_\odot$ may be real but is only barely significant at the 2-σ level. Statistical uncertainties in the current data prevent the reliable estimation of internal rotation at depths below $r = 0.2 R_\odot$. As we discuss below, these uncertainties will decrease with the acquisition of longer datasets.

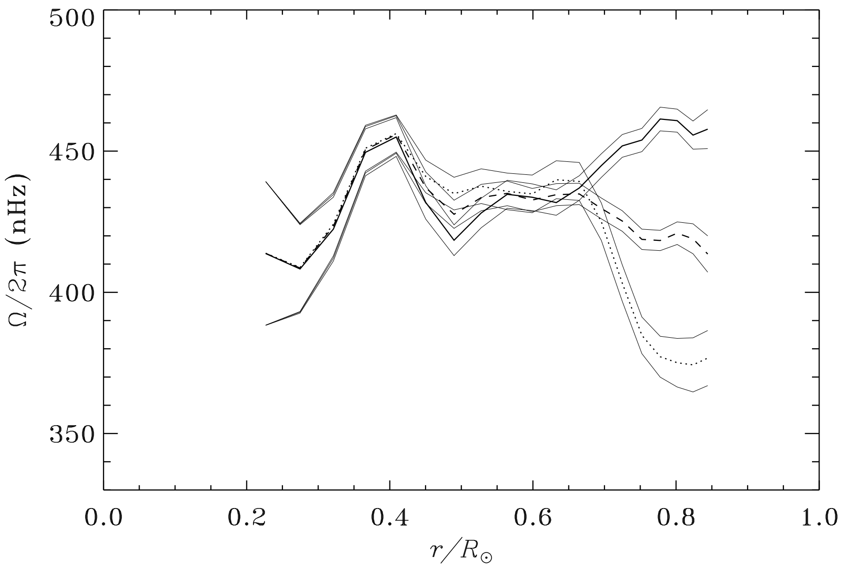

Fig. 4.— The inferred solar rotation rate as in Fig. 3a, at the equator (solid line), at colatitude 45° (dashed line) and at the pole (dotted line). One-sigma error levels are indicated by the thin solid lines.

In the deep interior ($r \lesssim 0.4 R_\odot$) our solution shows no variation with latitude. This is simply a reflection of the fact that below this depth we lose our ability to localize kernels at different latitudes. A averaging kernel corresponding to $r_0 = 0.4 R_\odot$, $\theta_0 = 90°$ is shown in Figure 5a; kernels for other target latitudes at this radius are indistinguishable from this one. This is a fundamental limitation imposed by the fact that the deepest interior is only sampled by low-degree p-modes, for which there are few different m values. Even with individual m splittings, rather than a coefficients, and a year-long set of observations, artificial experiments indicate that we will be unlikely to get substantially more resolution at this depth (Schou *et al.*, 1994). On the other hand, further out we can achieve some latitudinal resolution. As deep as $r_0 = 0.5 R_\odot$, for example, we are able to localize kernels at different latitudes (Figures 5b, 5c). Thus, if there were substantial latitudinal variation at $r_0 = 0.5 R_\odot$ we should be able to detect it. As can be seen from Figure 4, however, we see no significant variation with latitude anywhere in the radiative interior.

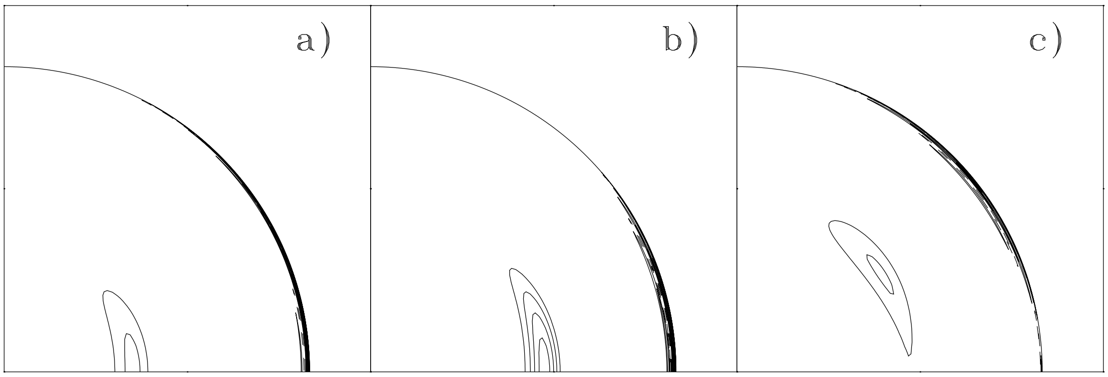

Fig. 5.— Averaging kernels corresponding to the inversion shown in Fig. 3a at the following target radii r_0 and target colatitudes θ_0: (a) $r_0 = 0.41R_\odot$, $\theta_0 = 90°$; (b) $r_0 = 0.56R_\odot$, $\theta_0 = 90°$; (c) $r_0 = 0.56R_\odot$, $\theta_0 = 45°$. In all cases the contour spacing is 4.0 (the kernels being dimensionless if r is measured in units of $R_\odot$). Positive contours are shown solid, negative contours dashed. For clarity the zero contour has been omitted.

5. Discussion

Solar models including only hydrodynamical mechanisms for angular momentum transport indicate that the presence of molecular weight gradients can inhibit the transfer of angular momentum out of the solar core (Pinsonneault *et al.*, 1989). These models indicate that the Sun can retain a large fraction of its initial angular momentum at depths $\lesssim 0.3R_\odot$ where these gradients become significant. While these models predict a rotation rate at 0.2 $R_\odot$ between approximately 10 and 30 times the surface equatorial rate, at depths $>0.4R_\odot$ the predicted rotation rate does not differ substantially from the surface rate. On the other hand, it has been suggested that a reasonably small (about 10^{-2} G) poloidal field in the solar radiative zone is sufficient to impose rigid rotation (Rosner and Weiss, 1985; Mestel and Weiss, 1987). The plausibility of this argument has been demonstrated by numerical simulations (Charbonneau and MacGregor, 1993). Past frequency splitting measurements have provided meaningful constraints on the rotation over only the outer half of the Sun and therefore have been unable to discriminate between these vastly different scenarios (Demarque & Guenther, 1988).

Our results indicate that the rather uniform rotation detected in the outer radiative interior extends down at least to $0.2R_\odot$. This measurement argues strongly against theories of solar angular momentum transport which predict large radial gradients in the solar interior angular velocity. While we cannot rule out rapid rotation below $0.2R_\odot$, the small radial extent of this region would require huge angular velocities to provide a significant reservoir of angular momentum.

The precision of these measurements is roughly consistent with theoretical limits imposed by the random nature of mode excitation (Duvall and Harvey, 1986; Veitzer *et al.*, 1992). We then expect that the errors of this measurement will decrease as the inverse square-root of the measurement duration. The LOWL observations are continuing and will eventually allow improved estimates of rotation at greater depths inside the Sun.

This work was partially supported by NSF through base funding of HAO/NCAR. We thank K. MacGregor, P. Charbonneau, T. Brown and J. Li for helpful discussions, and E. Yasukawa, D. Koon and D. Chu for collecting the observations.

REFERENCES

Brown, T.M. Christensen-Dalsgaard, J., Dziembowski, W.A., Goode, P., Gough, D.O. and Morrow, C.A., 1989, *ApJ*, **343**, 526.

Charbonneau, P. and MacGregor, K.B., 1993, *ApJ*, **417**, 762.

Christensen-Dalsgaard, J., and Schou, J., 1988, in *Seismology of the Sun and Sun-like Stars*, ESA Publications 286, Noordwijk, (E.J. Rolfe, ed.), 149.

Christensen-Dalsgaard, J., Gough, D.O., and Thompson, M.J., 1991, *ApJ*, **378**, 413.

Claverie, A., Isaak, G.R., McLeod, C.P., van der Raay, H.B. and Roca Cortés, T., 1981, *Nature*, **293**, 443.

Demarque, P. and Guenther, D.B., 1988, in *Seismology of the Sun and Sun-like Stars*, ESA Publications 286, Noordwijk, (E.J. Rolfe, ed.), 99.

Duvall, T.L. and Harvey, J.W., 1986, *Seismology of the Sun and the Distant Stars*, (D.O. Gough, ed.), D. Reidel, Dortrecht, 105.

Duvall, T.L., Harvey, J.W. and Pomerantz, M., 1986, *Nature*, **321**, 500.

Libbrecht, K.L., 1989, *ApJ*, **336**, 1092.

Loudagh, S., Provost, J., Berthomieu, G., Ehgamberdiev, S., Fossat, E., Gelly, B., Grec, G., Khalikov, S., Lazrek, M., Pallé, P., Régulo, C., Sanchez, L., Schmider, F.X., 1993, *A&A*, **275**, L25.

Mestel, L. and Weiss, N.O. 1987, *MNRAS*, **226**, 123.

Pallé, P.L., Pérez Hernández, F., and Roca Cortés, T., 1988, in *Seismology of the Sun and Sun-like Stars*, ESA Publications 286, Noordwijk, (E.J.Rolfe, ed.), 125.

Pallé, P.L., Régulo, C., and Roca Cortés, T., 1990, *Progress of Seismology of the Sun and Stars*, (Y. Osaki and H. Shibahashi, eds.), Lecture Notes in Phys. 367, Springer, Heidelberg, 189.

Pinsonneault, M.H., Kawaler, S.D., Sofia, S., and Demarque, P., 1989, *ApJ*, **338**, 424.

Rhodes, Jr., E. J. , Cacciani, A., Korzennik, S.G., Tomczyk, S., Ulrich, R.K. and Woodard, M.F., 1990, *ApJ*, **351**, 687.

Ritzwoller, M.H. and Lavely E.M., 1991, *ApJ*, **369**, 557.

Rosner, R. and Weiss, N.O., 1985, *Nature*, **317**, 790.

Schou, J. 1992, PhD Thesis, Aarhus universitet, Århus, Denmark.

Schou, J. 1994, in preparation.

Schou, J., Christensen-Dalsgaard, J. and Thompson, M.J., 1992, *ApJ*, **385**, L59.

Schou, J., Christensen-Dalsgaard, J. and Thompson, M.J., 1994, *ApJ*, **433**, 389.

Tomczyk, S., Streander, K., Card, G., Elmore, D., Hull, H. and Cacciani, A., 1994, *Sol. Phys.*, submitted.

Toutain, T., and Fröhlich, C., 1992, *A&A*, **257**, 287.

Toutain, T., and Kosovichev, A.G., 1994, *A&A*, **284**, 265.

Veitzer, S.A., Tomczyk, S., and Schou, J., 1992, in *GONG 1992: Seismic Investigation of the Sun and Stars*, PASP Conference Series, (T.M. Brown, ed.), **Vol. 42**, 465.

This preprint was prepared with the AAS LaTeX macros v3.0.